ISBN: 978-3-95450-216-5 doi:10.18429/JACoW-eeFACT2018-TUPAB02

LOW EMITTANCE BEAM TRANSPORT FOR e⁻/e⁺ LINAC

Y. Seimiya*, N. Iida, M. Kikuchi, T. Mori, KEK, Tsukuba, Japan

Abstract

Design luminosity of SuperKEKB is $8 \times 10^{35}\mathrm{cm}^{-2}\mathrm{s}^{-1}$, which is 40 times higher than that of KEKB achieved. To achieve the design luminosity, the beam have to be transported to the SuperKEKB main ring with the high bunch charge (4 nC) and low emittance: 40/20 μm for horizontal/vertical electron beam emittance and 100/15 μm for positron beam emittance in Phase 3 final. In the LINAC and the beam transport line, the emittance growth is mainly induced by residual dispersion, beam phase space jitter, wakefield in acceleration structure, and radiation excitation. In the Phase 2 operation, we have evaluated and, if possible, corrected these effects on the emittance. Results of the emittance measurement is described.

INTRODUCTION

SuperKEKB is e-/e+ collider for high energy particle physics in KEK. The design luminosity of SuperKEKB is 40 times higher than that of KEKB achieved [1]. This high luminosity can be realized by both doubling the current and making the beam size a one-twentieth compared with that of KEKB. The Phase 2 commissioning was finished in July 2018. The LINAC was developed for SuperKEKB [2]. During the operation in Phase 2, collimator tuning to reduce background of Belle-II detector, β squeezing for small beam size at the collision point, collision tuning to maximize the high luminosity, and so on have been done [3]. The physics run is scheduled to start in March 2019 as the Phase 3. Required beam-parameters for Phase 2 and Phase 3 (final) are shown in Fig. 1. In Phase 3 final, requirement to the beam charge is 4 nC for both beams. Required horizontal/vertical emittance is 100/15 μm for positron beam and 40/20 μm for electron beam. We have to convey this high-quality beam to the main ring without emittance degradation as far as possible. Otherwise, the injection rate would be worse and the luminosity would not be able to reach the target value.

A footprint of the LINAC and the beam transport line (BT) is shown in Fig. 2. The LINAC is composed of Sector A, B, J-ARC, C, and 1-5. The LINAC has two kinds of electron gun; a thermionic gun to obtain high-current beam used for positron production and a photocathode RF gun for low emittance electron beam. The large emittance of the positron beam emittance for LER is reduced by a damping ring (DR), which is placed beside the end of Sector 2. The beam is extracted from the end of Sector 2 to the LTR line at 1.1 GeV and injected to the DR. After two cycles of the LINAC pulse, the damped beam is, through the RTL line, resumed to the start of Sector 3 in the LINAC. Positron beam is accelerated up to 4 GeV and transported through the positron BT line and finally reaches the low energy ring (LER). Low emittance electron beam is accelerated up to 7 GeV and transported through the electron BT line and finally reaches the high energy ring (HER). To maintain the low emittance, fine tuning is necessary in every place of the system.

Stage	Phase 2 (Mar. – Jul. 2018)		Phase 3 (Mar. 2019 –)	
Beam	e+	e–	e+	e–
Bunch charge (nC)	1.5	1	4	4
Norm. Emit. (γβε) (μm)	200/40 (Hor./Ver.)	150	100/15 (Hor./Ver.)	40/20 (Hor./Ver.)
Energy spread	0.16%	0.1%	0.16%	0.07%

Figure 1: Required beam-parameters for SuperKEKB injector LINAC and the beam transport line.

SOURCES OF EMITTANCE GROWTH

We have evaluated several conceivable kinds of sources of the emittance growth.

Residual Dispersion

Through the residual dispersion, the energy spread converts to the beam size. First, an example of the dispersion correction at J-ARC section in the LINAC are shown in Fig. 3. where the horizontal axis shows path length along the beam line, blue and red lines show horizontal and vertical dispersion function, respectively. Before correction, large residual dispersion had emerged after the J-ARC as shown in the left inset of Fig. 3. By tuning the strength of quadrupole magnets, horizontal/vertical residual dispersion became small from 0.429/0.092 m to 0.024/0.017 m as shown in the right inset of Fig. 3.

In the same manner, we corrected dispersion in the RTL. In the RTL, there are two ARCs. For example, Fig. 4 shows before and after the dispersion correction in first ARC. The bottom figure in Fig. 4 shows residual dispersion. Blue and red lines show horizontal and vertical residual dispersion, respectively. After the dispersion correction, residual dispersion became smaller. Figure 5 shows values of residual dispersion before and after correction. In both ARCs, residual dispersion became smaller after the dispersion correction. But, the residual dispersion in the first ARC is still not small enough. We need more studies in detail on this issue.

Figure 6 shows improvement of the emittance due to dispersion correction. The emittance was measured with wire scanner (WS). First, we corrected the dispersion in the second ARC. By the correction, emittance was improved from

* seimiya@post.kek.jp

ISBN: 978-3-95450-216-5 doi:10.18429/JACoW-eeFACT2018-TUPAB02

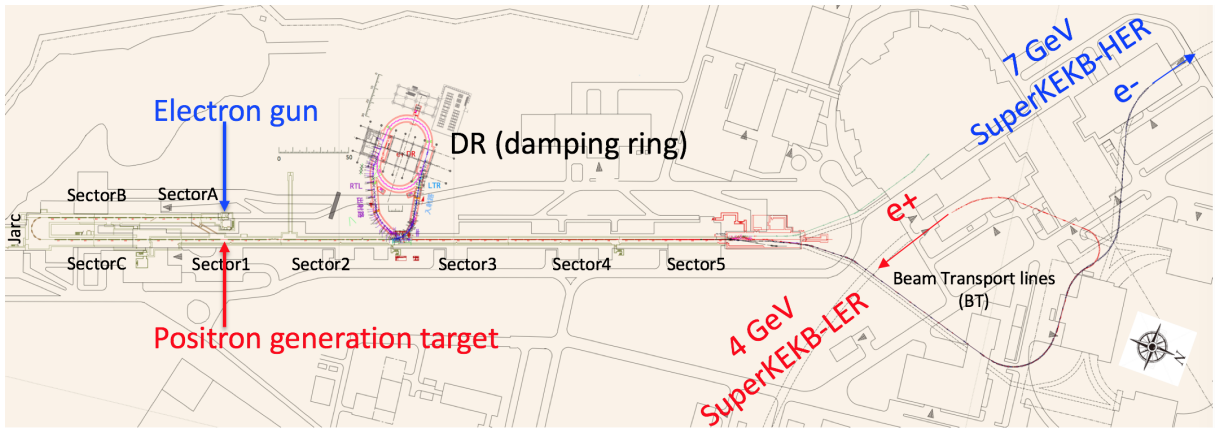

Figure 2: A footprint of SuperKEKB injector LINAC and the beam transport line.

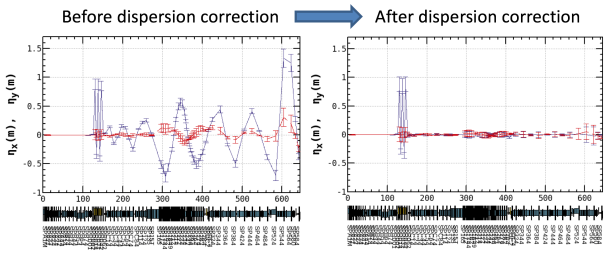

Figure 3: Dispersion measurement before and after the dispersion correction in the LINAC.

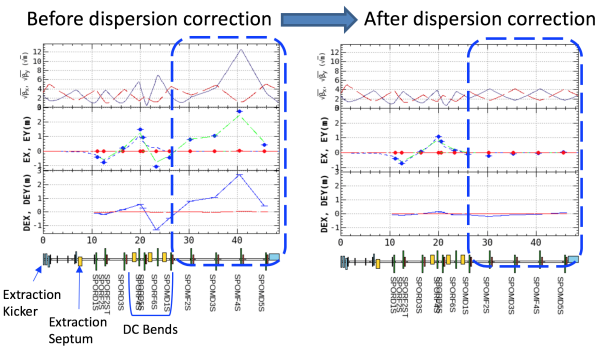

Figure 4: Dispersion measurement before and after the dispersion correction in the RTL.

about 300 μm to 200 μm. Then, we corrected the dispersion in the first ARC. By the correction, emittance was improved to 130 μm. Though the horizontal emittance became less than half, it is still twice as large as design value. Reference [4] mention this issue.

In the same manner, we corrected dispersion in each ARC of the BT. Figure 7 shows residual dispersion before and after correction for electron and positron beam. The order of ARC names are from the upstream to downstream of the BT. In the upstream of the WSs, dispersion correction was done. In some ARCs, dispersion correction is not completed.

e+	$<\eta x^2>^{1/2}$ [m]		$<\eta y^2>^{1/2}$ [m]		Fudge Factor of Quad.
Correction	Before	After	Before	After	[%]
2nd ARC	0.079	0.019	0.0094	0.0077	- 4.5
1st ARC	1.05	0.09	0.02	0.01	- 8.2

Figure 5: Residual dispersion before and after correction in the RTL.

e+ 0.7 [nC]	Horizontal Dispersion at Straight section after the Arcs				DR design emittance
	Before Correction	After Correction in 2nd arc	After Correction in 1st arc	Fudge Factor of Quads [%]	
$<\eta_x^2>^{1/2}$ [m]	0.079	0.019		- 4.5	
	1.05		0.09	- 8.2	
Measured Emittance in Sector 3					
$\gamma\beta\varepsilon_x$ [μm]	293±44.5	192±22.4	126±8.2		64.3
$\gamma\beta\varepsilon_y$ [μm]	1.84±0.163	2.01±0.363	1.5±0.1		

Figure 6: Emittance improvement due to dispersion correction.

Beam Phase Space Jitter

The extent of the transported beam to the main ring must be stable so that the beam can be injected inside the main ring acceptance. The emittance that includes beam phase space jitter, called as effective emittance, must be satisfy the requirement. We evaluated the emittance growth due to the beam phase space jitter and investigated their sources.

To evaluate the emittance growth due to beam phase space jitter, we introduce following effective emittance,

$$\epsilon_{eff} = \sqrt{\langle X^2\rangle \langle X'^2\rangle - \langle XX'\rangle^2} = \sqrt{\epsilon_0^2 + \epsilon_j^2 + 2\epsilon_0\epsilon_j B_{mag}},$$

where

$$X = x + \Delta x,\ X' = x' + \Delta x',$$
$$\epsilon_0 = \sqrt{\langle x^2\rangle \langle x'^2\rangle - \langle xx'\rangle^2},$$
$$\epsilon_j = \sqrt{\langle \Delta x^2\rangle \langle \Delta x'^2\rangle - \langle \Delta x \Delta x'\rangle^2},$$
$$B_{mag} = \frac{\gamma_0\beta - 2\alpha_0\alpha + \beta_0\gamma}{2},$$

ISBN: 978-3-95450-216-5 doi:10.18429/JACoW-eeFACT2018-TUPAB02

e-	<ηx²>^1/2 [m]		<ηy²>^1/2 [m]		Fudge Factor of Quadrupole	
Correction	Before	After	Before	After	[%]	
Slope 1	0.13	0.11	0.05	0.01	1.0~5.9	BT-WS placed
Bte 0th ARC	0.11	0.02	0.01	0.02	0~6.7	
Bte 1st ARC	0.102	0.038	0.029	0.036	2.37	
Bte 2nd, 3rd ARC	0.066	0.029	0.037	0.034	2.52	
Slope 2	0.104	0.091	0.192	0.116	3.55	Inj. point to MR
Bte 4th ARC	-	-	-	-	-	

e+	<ηx²>^1/2 [m]		<ηy²>^1/2 [m]		Fudge Factor of Quadrupole	
Correction	Before	After	Before	After	[%]	
BTp 0th ARC	0.27	0.02	0.01	0.03	-26~12.9	BT-WS placed
BTp 1st ARC	0.037	0.047	0.126	0.102	2.5	
Slope 1	-	-	-	-	-	
BTp 2nd, 3rd ARC	-	-	-	-	-	
Slope 2	-	-	-	-	-	Inj. point to MR
BTp 4th ARC	-	-	-	-	-	

Figure 7: Residual dispersion before and after correction for both electron and positron beam in the BT.

ϵ_0 and ϵ_j are nominal emittance and emittance growth induced by beam phase space jitter (jitter emittance), respectively. B_{mag} is a phase space mismatch between the beam and the jitter. The value is equal to or larger than 1. If $B_{mag} = 1$, there is no mismatch and the effective emittance equals just the nominal emittance plus the jitter emittance. B_{mag} is measured to be about 1-2 in the usual LINAC operation, which is measured with WS. From the beam position, assuming the transfer matrix between two BPMs, beam angle can be estimated. Jitter emittance can thus be derived from the beam position jitter and beam angle jitter.

We have measured the beam position jitter at BPM in the LINAC. Figure 8 shows the beam position jitter and the jitter emittance. Horizontal axis shows the path length after the electron gun. Position jitter is defined as standard deviation of measured beam position. Around the 140 m point of the figure, there is J-ARC section. Because the J-ARC section is dispersive, beam energy jitter is converted to beam position jitter in this section. Dispersion and position jitter were about 0.8 m and 360 μm at the center of this section, respectively, then energy jitter is estimated to be about 0.045%. In addition to the J-ARC, behind the positron target placed in about 290 m point, beam position jitter and jitter emittance were observed to increase as shown in the left figure in Fig. 8. In this case, horizontal/vertical jitter emittance was about 28/7 μm at the end of the LINAC. Target value of the horizontal/vertical emittance in Phase 3 is 40/20 μm. Therefore, the effect of jitter emittance on effective emittance was very large. On the other hand, after the dispersion correction, horizontal/vertical jitter emittance was decreased to about 1.8/0.9 μm at the end of the LINAC as shown in the right figure in Fig. 8. Beam phase space jitter was successfully reduced by the dispersion correction. Small emittance growth still remains behind the target even after the correction. This result is obtained in case of 1 nC, therefore we should understand origin of the beam phase space jitter to prepare for the 4 nC beam.

Wakefield in Acceleration Structure

Wakefield, generated by a head of bunch, kicks its own tail. Thus if the beam is off-centered in the structure, the transverse wakefield increases beam emittance. This effect can

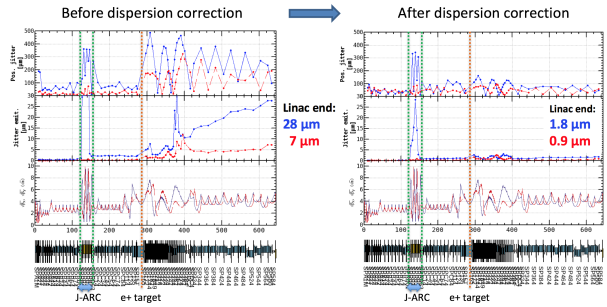

Figure 8: Measured beam position jitter and jitter emittance in the LINAC before and after dispersion correction. The electron beam was 1 nC and generated by RF gun.

Table 1: Basic Parameter Set

Parameter	Value	Unit
Initial emittance	10	μm
Initial bunch length	3/2.35	mm
Initial energy spread	0.004	–
Charge	5	nC
Distribution	Gaussian	–
S-band acc. cavity aperture	ϕ20	mm

be minimized by a proper orbit correction. We performed particle tracking simulation to evaluate emittance growth induced by wakefield in acceleration structure. The particle tracking is simulated by the SAD program [5]. Misalignment of the components had been measured by laser-based alignment system [6, 7]. The measured misalignment values were used for this simulation. Table 1 shows basic parameter set of the simulation. Left figure in Fig. 9 shows emittance after orbit displacement was minimized. Blue and red dots show horizontal and vertical emittance, respectively. Blue and red lines show the horizontal and vertical requirements for Phase 3, respectively. As the beam went down to the LINAC end, the horizontal/vertical emittance grew up to 240/120 μm at the end of the LINAC. On the other hand, right figure in Fig. 9 shows emittance minimized at the end of the LINAC. Emittance growth, in this case, occurred at Sector C and corrected at Sector 2. By an orbit correction for emittance preservation, emittance growth induced by an accelerator structure could be cancelled by the other accelerator structure. In this case, the horizontal/vertical emittance is 22/11 μm at the end of the LINAC. These emittances are less than Phase 3 requirements. Especially, the vertical emittance is almost same as initial emittance. In the simulation, transmission rate was almost 1.

Radiation Excitation

Radiation excitation effect on emittance is proportional to both Lorenz gamma to the fifth power and inverse of curvature radius to the third power. Especially, electron beam (7 GeV) is strongly affected by the radiation excitation effect. Particle tracking was performed from beginning to end of the BT. Figure 10 shows the simulation results. Initial

ISBN: 978-3-95450-216-5 doi:10.18429/JACoW-eeFACT2018-TUPAB02

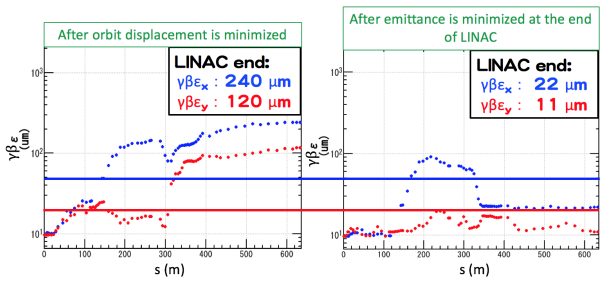

Figure 9: Emittance change due to different orbit correction in the LINAC.

Radiation excitation effect on emittance	Initial particles	With Radiation	Phase-III final requirement
e- (7 GeV) $\gamma\beta\varepsilon_x$ [μm]	20	69	40
e+ (4 GeV) $\gamma\beta\varepsilon_x$ [μm]	64	77	100

Figure 10: Radiation excitation effect on emittance in the BT.

horizontal emittance of electron/positron beam is 20/64 μm. These emittances are increased by radiation excitation and reach 69/77 μm at the end of the BT. Especially, electron beam emittance at the end of the BT is larger than Phase 3 requirement. We are reconsidering the requirement by taking into account of the actual injection system and beam optics.

EMITTANCE MEASUREMENT

First, we show emittance measurement result of electron beam as Fig. 11. Left and right figures show horizontal and vertical emittance measured at each sector, respectively. Purple dots show emittance of electron beam generated with thermionic gun. Green and blue dots show emittance of electron beam generated with RF gun. Green dots measured in 29 June 2018 and blue dots measured in the next day. Clearly, beam emittance with the RF gun was smaller than that with thermionic gun. Blue and orange dashed lines show Phase 2 and Phase 3 requirement value, respectively. The requirement emittance of electron beam at the end of the LINAC is satisfied for Phase 2, but not for Phase 3. Currently, we performed orbit correction algorithm only to reduce orbit distortion. We will introduce the orbit correction program for emittance preservation in this Winter. Large emittance growth was observed at the BT though dispersion correction was done. This emittance growth is irrelevant to radiation excitation because used WSs in the BT are placed where the total bending angle from the beginning of the BT is small.

Finally, we show emittance measurement result of positron beam in Fig. 12. In Phase 2, the requirement emittance of positron beam at the end of the LINAC was also satisfied though the requirement for Phase 3 was also not satisfied. Emittance was also increased in the BT though dispersion correction was done. Investigations for these unknown emittance growth sources in the BT are in progress.

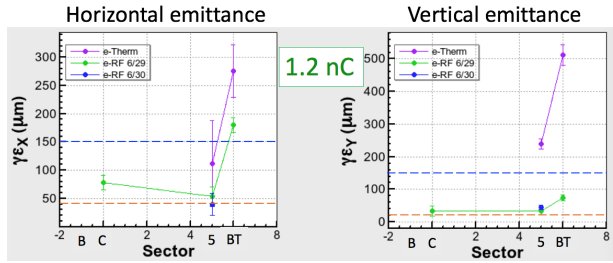

Figure 11: Emittance measurement result for electron beam at each sector.

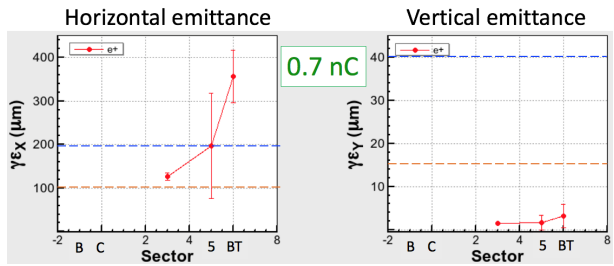

Figure 12: Emittance measurement result for positron beam at each sector.

SUMMARY

In the LINAC and the BT, transport of high current and low emittance beam is necessary for SuperKEKB. In the LINAC, emittance requirement for Phase 2 was satisfied after applying dispersion correction, reduction of beam phase space jitter, and orbit correction. To suppress the emittance growth more, automatic orbit correction for minimizing emittance growth is desired. We plan to introduce such an emittance control program in this Winter. Large emittance growth was observed in the BT. Emittance requirement in Phase 2 was not satisfied in the BT. Investigations of the issues are in progress.

ACKNOWLEDGEMENTS

This work was partly supported by JSPS KAKENHI Grant Number 16K17545.

REFERENCES

[1] Y. Funakoshi *et al.*, "Achievements of KEKB", *Prog. Theor. Exp. Phys.* 03A001 (2013).

[2] K. Furukawa *et al.*, "KEKB Injection Developments", in Proc. of eeFACT2018, Hong Kong, China, paper TUPAB01, this conference.

[3] Y. Ohnishi *et al.*, "Highlights from SuperKEKB Phase 2 Commissioning", in Proc. of eeFACT2018, Hong Kong, China, paper MOXAA02, this conference.

[4] N. Iida *et al.*, "Commissioning of Positron Damping Ring and Beam Transport for SuperKEKB", in Proc. of eeFACT2018, Hong Kong, China, paper TUPAB07, this conference.

ISBN: 978-3-95450-216-5 doi:10.18429/JACoW-eeFACT2018-TUPAB02

[5] "Strategic Accelerator Design (SAD) home page", http://acc-physics.kek.jp/SAD/

[6] Y. Seimiya *et al.*, "Emittance growth by misalignments and jitters in SuperKEKB injector LINAC", in *Proc. of IPAC2016*, Busan, Korea, paper THPOR040 (2016).

[7] T. Suwada *et al.*, "Real-time observation of dynamic floor motion of the KEKB injector linac with a laser-based alignment system", *PRST-AB*, 20, 033501 (2017).